



# Study of inks used in biomedical optics phantoms: stability and ageing

P.A. Pardini,<sup>a</sup> M.V. Waks Serra,<sup>a\*</sup> H.F. Ranea-Sandoval,<sup>b</sup> J.A. Pomarico<sup>a</sup> and D.I. Iriarte<sup>a</sup>

<sup>a</sup>IFAS – CIFICEN (UNCPBA – CONICET), Pinto 399 (7000) Tandil, Argentina. E-mail: [mwwaks@exa.unicen.edu.ar](mailto:mwwaks@exa.unicen.edu.ar)

<sup>b</sup>IFAS, UNCPBA, Pinto 399 (7000) Tandil, Argentina

Inks are the most common absorbers added in phantoms for biomedical optics experiments. Due to the small quantities required, it is usual to prepare dilutions in distilled water and to store them for future use. However, they may degrade with time. This work investigates the stability, over a 60-day period, of various types of ink dilutions as a component used in tissue-mimicking phantoms. For this purpose, the optical properties, particularly the absorption coefficient, of a diffusive phantom fabricated with various pre-diluted inks have been determined using time-resolved experiments, for the period of time under investigation. Two commercial India inks were studied, namely Rotring® and Higgins®, as well as a third type, a black ink-jet printer ink (Powertec®). Results suggest that all ink dilutions suffer from ageing, affecting the reproducibility of the optical properties of the phantoms. For the investigated period, this effect was more noticeable for the India inks, but almost negligible for the ink-jet printer ink.

**Keywords:** NIR spectroscopy, biomedical optics, India ink, absorption coefficient

## Introduction

In the last few decades, the study of light propagation in turbid media, such as biological tissue, has achieved significant prominence. The use of red and near infrared (NIR) radiation has been proposed as a tool for possible non-invasive techniques, for instance diffuse optical tomography (DOT) and quantitative photoacoustic imaging.<sup>1–5</sup>

In the case of DOT, the interest relies on its ability to localise inhomogeneities and to characterise them optically, and to obtain functional information of organs (oxygenation, vascularisation, etc.), thus complementing the well-established techniques, e.g. X-ray tomography, magnetic resonance imaging, ultrasound imaging, positron emission tomography, among others.<sup>6–10</sup> Often, DOT is complemented with the use of fluorescent contrast agents, like indocyanine green.<sup>11</sup>

The optical properties of interest for biological tissue diagnoses are the absorption coefficient  $\mu_a$ , which is the reciprocal of the mean path travelled by a photon before it is absorbed, and the reduced scattering coefficient defined as  $\mu'_s = \mu_s(1 - g)$ , which is the inverse of the transport mean free path. The

parameter  $\mu_s$  is the scattering coefficient, representing the inverse of the mean path between collisions, and  $g$  is the anisotropy factor,<sup>12</sup> giving the average value of the scattering angle. In the diffuse regime, which is the case of NIR light propagating in tissue, scattering dominates over absorption and the process is described by the diffusion approximation of the radiative transfer equation.

The evaluation of these parameters is usually performed using phantoms, which are tissue-like constructions of known geometry and composition, and are commonly used in the development and characterisation of imaging systems and reconstruction algorithms. These phantoms can be either solid or liquid. The solid ones are commonly made of resins, plastics or gels, while liquid ones are fabricated with a mixture of distilled water, a scattering agent, such as Intralipid® or milk, and an absorber agent, generally pre-diluted India ink.<sup>13,14</sup> Liquid phantoms present several advantages, including reproducibility and ease of gradually changing the optical properties and varying the position of inclusion(s).

An appropriate protocol for phantom construction is fundamental, and good calibration of the optical properties is required. It is usual for the tissue optics community to use pre-diluted solutions of ink over long periods of time, relying on the long-term stability of these solutions.<sup>14</sup> As we show, this is not always the case, and some changes of the optical absorption can occur due to relatively long periods of storage of diluted inks.

With this as a motivation, we studied the temporal behaviour of an absorber agent for liquid phantoms made of milk and distilled water. The optical properties of the phantom,  $\mu_a$  and  $\mu'_s$ , were measured employing the time resolved approach in a transmission geometry at 785 nm. The study was performed over two months and for two different types of inks, namely India ink, commonly employed for biomedical phantoms,<sup>13,15,16</sup> and a commercial black ink-jet printer ink, which, to our knowledge, has not been reported before for this purpose. In particular, the absorption coefficient can be defined as the product of an intrinsic or specific absorption,  $\epsilon$ , and the concentration of absorbers,  $\rho$ , namely  $\mu_a = \epsilon\rho$ . Di Ninni *et al.*<sup>13</sup> demonstrated that the specific absorption coefficient of non-diluted India inks keeps constant over time. Based on this statement, we propose that if  $\mu_a$  varies with time, any discrepancy with the expected values can be ascribed to alterations in the concentration of absorbers in the dilutions.

We show that storing ink dilutions between their preparation and their use in an experiment does produce a reduction in the absorption coefficient,  $\mu_a$ , relative to its value (for a fixed volume of dilution) measured immediately after preparation of the dilution, ascribing this reduction in  $\mu_a$  to sedimentation of the intrinsic absorbers.

The paper is organised as follows. In the next section we introduce the theoretical aspects of our proposal; in the section after that we describe the entire experimental procedure and protocol. Then we present and discuss the main results, and in the final section we present a summary of the most important conclusions.

## Theoretical considerations

For determining the optical properties of a phantom in the time resolved approach, we used the theoretical model developed for slabs in the work of Contini *et al.*<sup>17</sup> to fit the distributions of time of flight (DTOFs) resulting from experiments. The expression for the diffuse transmittance  $T(s, \rho, t)$ <sup>17</sup> per unit time and unit area, for a slab of thickness  $s$ , reduced scattering coefficient  $\mu'_s$  and absorption coefficient  $\mu_a$ , for a medium that fulfils the diffusion approximation (i.e.  $\mu'_s \gg \mu_a$ ), is the following:

$$T(s, \rho, t) = \frac{\exp[-\mu_a vt - \rho^2 / 4Dvt]}{2(4\pi Dv)^{3/2} t^{5/2}} \times \sum_{m=-\infty}^{+\infty} \left[ z_{1,m} \exp\left(-\frac{z_{1,m}^2}{4Dvt}\right) - z_{2,m} \exp\left(-\frac{z_{2,m}^2}{4Dvt}\right) \right] \quad (1)$$

where  $\rho$  is the source–detector distance,  $D = (3\mu'_s + \mu_a)^{-1} \approx (3\mu'_s)^{-1}$  is the diffusion coefficient,  $v = cn^{-1}$  is the speed of light in the medium,  $z_{1,m} = s(1 - 2m) - 4mz_e - z_0$  and  $z_{2,m} = s(1 - 2m) - (4m - 2)z_e + z_0$ . For a refractive index of  $n = 1.4$ ,  $z_e \approx 2.05(\mu'_s)^{-1}$ , which is the extrapolated distance where the diffuse intensity  $U(r)$  vanishes.<sup>18</sup>

The measured DTOFs, together with the corresponding instrument response function (IRF), are given as input for a Levenberg–Marquardt routine, implemented in Python, which in turn gives the set of optical parameters that minimises quadratic errors.<sup>17</sup>

Briefly the fitting procedure goes through the following steps:

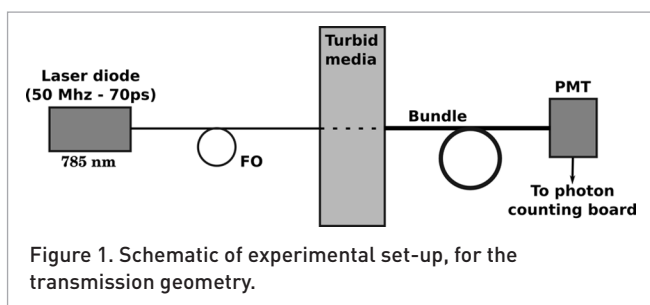
- The IRF of the measurement equipment was obtained. This can be done by removing the phantom in the experimental set-up of Figure 1, and thus the measured curve represents the laser pulse broadening due to all other components (optical fibres, PMT, electronics, etc.) but the phantom itself.
- Using initial guess values for the optical parameters, the IRF is convolved with a curve obtained from the theoretical model of equation (1) and the result is compared to the experimental DTOF.
- Step (b) is repeated for different values of the parameters in the Levenberg–Marquardt routine until the desired convergence is reached.

This time resolved technique requires a non-linear fitting procedure to obtain the optical properties, but, as compensation, it enables both optical parameters to be obtained simultaneously. There are other simpler techniques that can be performed, such as collimated transmittance; however, this gives information about the extinction coefficient, which has both absorption and (single) scattering coefficients entangled, thus demanding a complementary measurement in order to obtain the absorption coefficient<sup>13</sup> of interest for this particular work.

## Materials and methods

Measurements were carried out on liquid phantoms, fabricated with distilled water, commercial whole milk with 3% fat as the scattering agent and pre-diluted ink as the absorber. The proportion of water and milk was kept fixed, at such a value so as to emulate the reduced scattering coefficient of biological tissues (about  $1 \text{ mm}^{-1}$ ),<sup>19</sup> and the ink proportion was varied by adding fixed volumes of ink dilutions to produce variations in the absorption coefficient.

The experimental set-up is shown in Figure 1. The laser source, a Becker & Hickl system (BHLP-700; <http://www.becker-hickl.com/pdf/redlaser3.pdf>), operating at 785 nm and 50 MHz, produced pulses of 70 ps, and an average power of 1 mW. It illuminated via a 600  $\mu\text{m}$  diameter optical fibre the phantom contained in a 4 cm glass cuvette. The light emerging at the opposite face of the phantom was collected by a 0.8 cm diameter optical fibre bundle, which was mounted coaxially

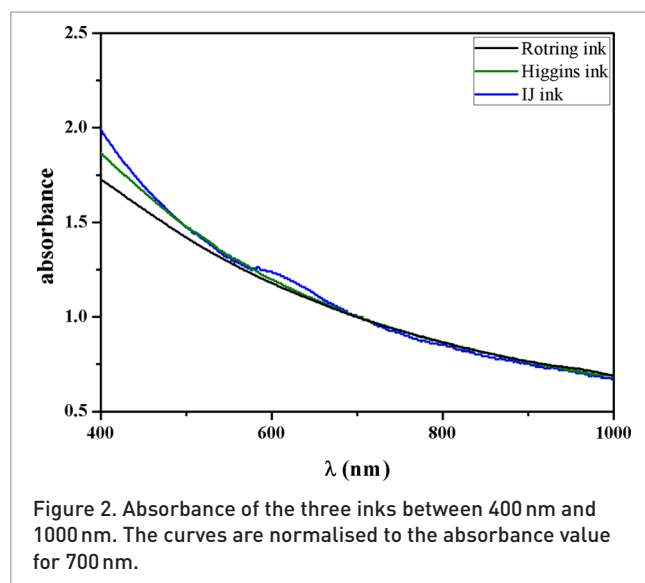


to the source fibre, and carried to a photomultiplier (Becker & Hickl PCM-100-20). Its electrical output was connected to a time-correlated single-photon counting board (Becker & Hickl SPC 130) in a computer, where the resulting DTOFs were measured and stored. To obtain the optical properties of the phantom for each ink concentration, the obtained DTOFs were fitted to the theoretical model, as previously described.

Since the main goal of this work was to determine possible variations of the diluted ink absorption with storage time, revealed through variations of the absorption coefficient, we first evaluated the time-stability of our equipment. To this end, we carried out test experiments by performing several measurements on both a solid phantom made of resin and a liquid phantom, during a complete working day. The statistics over 40 measurements gave, for the solid phantom, an average value of  $\mu_a = 0.00326 \pm 0.00006 \text{ mm}^{-1}$  and  $\mu'_s = 0.621 \pm 0.003 \text{ mm}^{-1}$ , while for the liquid phantom we obtained  $\mu_a = 0.0086 \pm 0.0001 \text{ mm}^{-1}$  and  $\mu'_s = 0.698 \pm 0.009 \text{ mm}^{-1}$ . From these data, we obtained that the systematic error in the determination of the optical parameters never exceeds 2%.

As already stated, we worked with three commercially available inks, two of the type known as India ink, namely Rotring® (<http://www.rotring.com/en/>) and Higgins® (<http://www.higginsinks.com>), and one black ink-jet printer (IJ) ink, namely Powertec® HP PIG 4844 black, specially manufactured for Hewlett-Packard printers (<http://www8.hp.com/cl/es/products/oas/product-detail.html?oid=12882>). In order to evaluate the feasibility of the IJ ink we measured the absorbance of all three inks, between 400 nm and 1000 nm, using a spectrophotometer (Shimadzu UV-1800, <http://www.shimadzu.com>). The absorbance curves are depicted in Figure 2, showing a similar behaviour for all inks, which indicates the suitability for their use for wavelengths in the NIR region.

To achieve reproducibility we adopted the following procedure. At day 0, we prepared the three ink dilutions, mixing each ink in fresh distilled water, in proportions of 1:1000 for the Rotring® ink and 3:1000 for the other two, to equate the values of  $\mu_a$  with the same added volume of dilution. This procedure is required because, first, the volume of undiluted ink needed for the phantoms is about 1–2  $\mu\text{L}$  per litre of final mixture, and, second, the ink is not easily diluted, and a mixing process is mandatory to obtain a homogeneous preparation. The dilutions were made in plastic bottles, after cleaning them with distilled water and subsequent drying. The bottles



containing the dilutions were then submerged in an ultrasonic bath at room temperature for 30 min. The same dilutions were used throughout the 60 days of the experiments and the ultrasonic mixing was repeated prior to each measurement to avoid agglutination, with a consequent change in the intrinsic absorption. During the complete period of the experiments the laboratory temperature was kept between 22 °C and 25 °C by air conditioning.

Each measurement series consisted of the following three steps:

- (1) to prepare the mixture of distilled water and milk (fresh for every measurement day),
- (2) to obtain the optical properties without any ink added and
- (3) to obtain the new optical properties after adding a constant volume of the corresponding ink dilution. Dilution volumes added per litre of phantom were  $\Delta V_{\text{ink}}/V = 2.5 \text{ mL L}^{-1}$  per step (this corresponds to steps of  $1 \mu\text{L L}^{-1}$  for the Rotring® ink and  $3 \mu\text{L L}^{-1}$  for the other two inks).

This last step was repeated, increasing the added amount of ink dilution until  $\mu_a$  reached approximately  $0.02 \text{ mm}^{-1}$ , which is about twice the value usually given for healthy tissue.<sup>19</sup> The DTOF corresponding to each single concentration was measured three times and the results were averaged. The entire protocol was then repeated at different days up to a maximum of 60.

In general, a linear increment in the absorption coefficient and a negligible variation in the reduced scattering coefficient are desired with increasing ink concentration. This assumption will be compared with the results of our experiments.

## Results and discussion

After 60 days from the dilutions being prepared, we took pictures of the plastic bottles placed upside down after ultrasonic mixing. These are shown in Figure 3, where it is clearly seen that both India ink dilutions presented a relatively high



Figure 3. Receptacles of ink dilutions after 60 days, after ultrasonic mixing procedure (the large spots in the IJ container are droplets of the dilution).

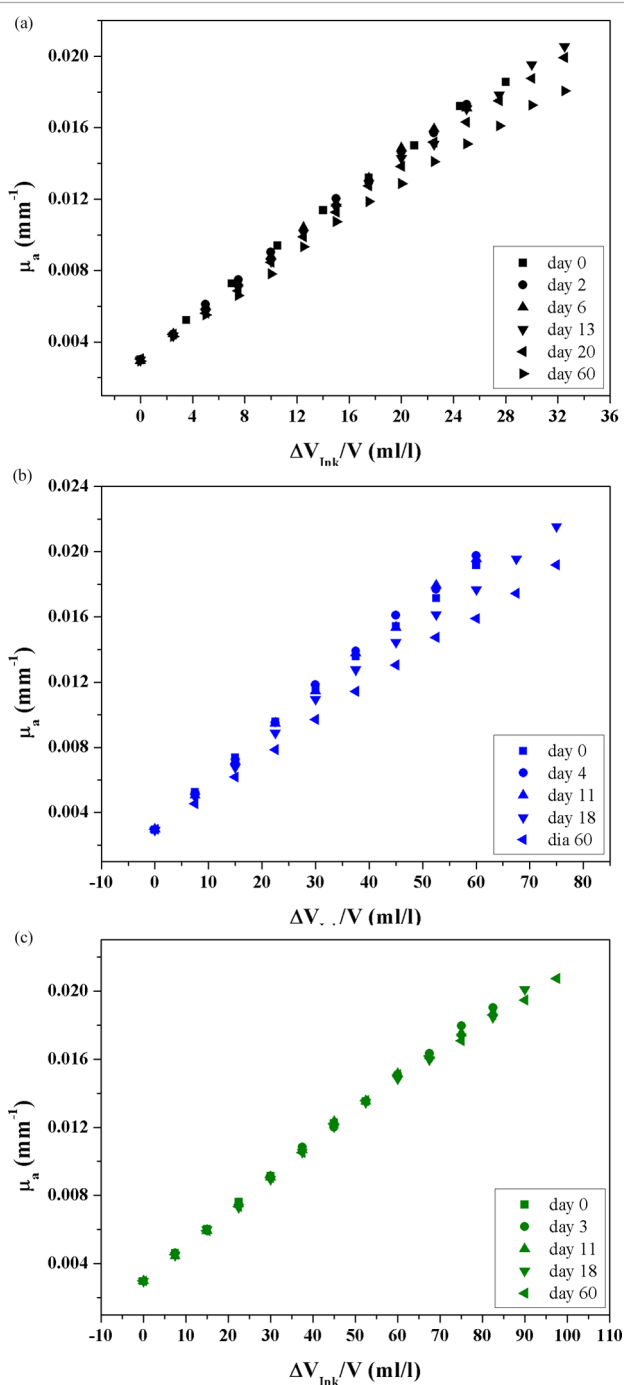


Figure 4. Absorption coefficient versus added ink volume after various numbers of days, showing the ageing of the ink dilutions. (a) Rotring® ink. (b) Higgins® ink. (c) IJ ink.

degree of sedimentation, persistent even after the mixing process, which was not the case for the IJ ink dilution, for which sedimentation was almost imperceptible.

In Figure 4 we present the results corresponding to the variation of the absorption coefficient with increasing added ink. As desired,  $\mu_a$  shows a linear increase with ink volume independent of the ink used. However, some differences between inks are worth mentioning. Both India inks [Figure 4(a) and (b)] showed a measurable decrease in the slope of the curves with ageing of the dilutions. This decrease was unnoticeable for the IJ ink. Considering this and Figure 3, and assuming that the absorbing particles are homogeneously distributed and there is negligible evaporation, it can be stated that the number of absorbing particles per unit volume in suspension decreases with storage time, due to sedimented particles attached to the bottom of the receptacles. This conclusion is also evident from Table 1, in which the resulting numerical values and the corresponding error in the slope of curves of  $\mu_a$  versus  $\Delta V_{ink}/V$  for the three inks are given.

From Figure 4 and Table 1 we can conclude that, in the period of 60 days for which the experiment lasted, the slope of the absorption coefficient using the ink dilution from Rotring® reduces by 18%, the absorption coefficient resulting when using the ink dilution from Higgins® decreases by 21%, while the dilution prepared with the IJ ink does not show a clearly decreasing tendency.

In Figure 5 the absorption coefficient versus the storage time of the ink dilution for all inks used is presented for a fixed volume of added ink, which gives a value of  $\mu_a$  close to  $0.01 \text{ mm}^{-1}$  (filled symbols), typical for mammalian tissue,<sup>19</sup> and, as a comparison, for the phantom without ink (open symbols). It is evident that for this phantom the absorption coefficient remains almost constant. This remarkable low dispersion in the values of  $\mu_a$  clearly shows both the high reproducibility of the liquid phantom and the stability of the time resolved measurements over relatively long periods of time for this parameter.

As already mentioned, according to the results of Di Ninni *et al.*,<sup>13</sup> the specific absorption coefficient,  $\epsilon_a$ , is defined by  $\mu_a = \epsilon_a \rho$ , where  $\rho$  is the concentration of absorbers in the ink solution, and  $\epsilon_a$  remains constant for India inks. The parameter  $\epsilon_a$  is directly related to the slope of  $\mu_a$  versus  $\Delta V_{ink}/V$ , as presented in Table 1. It must be noted that in the present work, the parameter of interest is not  $\epsilon_a$  but the absorption coefficient,  $\mu_a$ . Referring again to Figure 3, and as noted before, the concentration of ink absorbers in colloidal suspension decreases with time as a result of sedimentation effects. As a

Table 1. Slopes of the plots in Figure 4 in mL/L.

Rotring®		Higgins®		IJ ink	
Day	Slope ( $\times 10^{-4}$ )	Day	Slope ( $\times 10^{-4}$ )	Day	Slope ( $\times 10^{-4}$ )
0	$5.58 \pm 0.06$	0	$2.68 \pm 0.03$	0	$1.98 \pm 0.02$
2	$5.68 \pm 0.05$	4	$2.81 \pm 0.03$	3	$1.99 \pm 0.02$
6	$5.74 \pm 0.04$	11	$2.79 \pm 0.02$	11	$1.97 \pm 0.02$
13	$5.47 \pm 0.04$	18	$2.48 \pm 0.02$	18	$1.93 \pm 0.02$
20	$5.13 \pm 0.04$	60	$2.21 \pm 0.02$	60	$1.99 \pm 0.02$
60	$4.73 \pm 0.04$				

consequence, if equal volumes of the dilution are added to the phantom at different days, they will not contain an equal effective number of absorbers, producing the observed decrease in the absorption coefficient  $\mu_a$  with time (Figure 5).

The variation of concentration of absorbers added,  $\rho_i$  (with  $i$  numbering the day), relative to that of the first day,  $\rho_0$ , can be estimated from the ratio between the corresponding absorption coefficients, according to the definition of  $\epsilon_a$ . Thus,  $\rho_i/\rho_0 = \mu_{ai}/\mu_{a0}$ , and Figure 6 shows how this relation decreases with time. This change was significant for phantoms prepared with the India inks, while it was almost negligible for that with IJ ink.

As the absorption coefficient obtained for the phantoms with IJ ink was more stable with time, it was of great interest to study the behaviour of the reduced scattering coefficient. Figure 7 shows  $\mu'_s$  against  $\mu_a$  for several experiments performed during the two-month study period. We chose to plot  $\mu_a$  instead of added ink volume on the x-axis so as to avoid errors in the concentration of absorbers, due to the sedimentations mentioned before (this does not imply a dependence between the two coefficients). Even if the milk used came from the same manufacturer, it may be of different batches; this can lead to small differences in the initial  $\mu'_s$ . Thus we normalised the curves to their own maximum.

The dispersion observed is of the order of 2%, around an average value of  $0.98 \text{ mm}^{-1}$ , comparable to the  $\mu'_s$  determination error calculated before. So, as expected, the addition of IJ ink did not significantly alter the scattering.

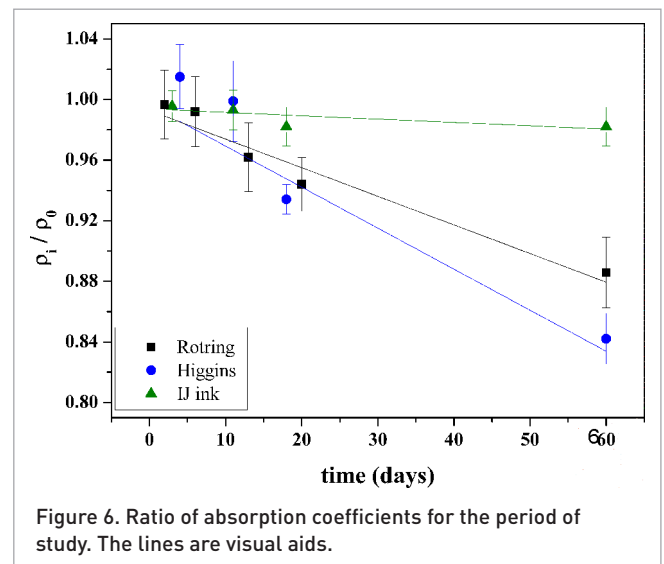


Figure 6. Ratio of absorption coefficients for the period of study. The lines are visual aids.

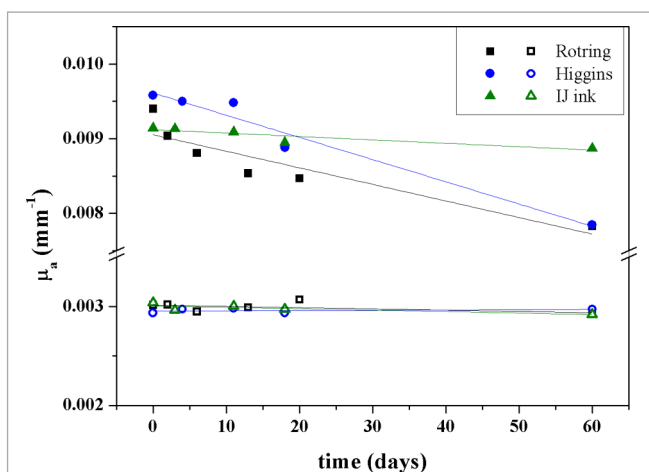


Figure 5. Evolution of absorption coefficients during the 60-day period, for no-ink phantom (open symbols) and a fixed volume of added ink (filled symbols). The straight lines are linear fits.

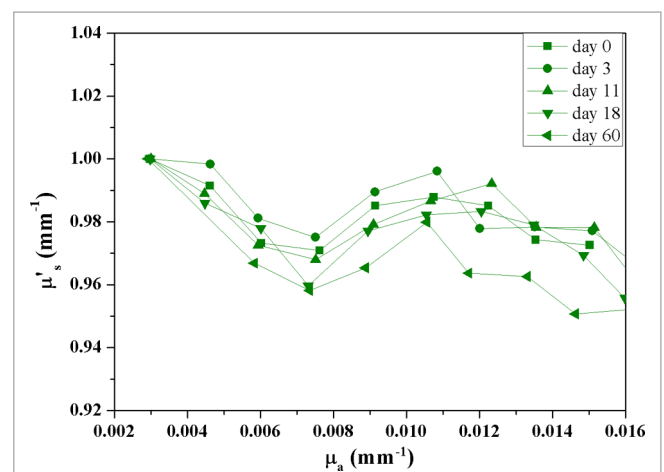


Figure 7. Reduced scattering coefficient (normalised to the maximum) versus absorption coefficient for IJ ink for various numbers of days.

## Conclusions

A complete study of the absorption coefficient of liquid phantoms, fabricated with distilled water, whole milk and pre-diluted inks, from three different commercial sources, has been described. Special attention has been paid to the behaviour of ink dilutions with time, through a period of two months.

From the results presented, we can conclude that the three inks used in this work (Rotring®, Higgins® and Powertec®) are suitable for phantom fabrication, but it is recommended to measure the optical properties on each day of work and to not assume them based on a previous calibration. Moreover, the IJ ink showed a high stability, within the determination error, for at least two months, and it is thus worth using this type of ink if a dilution is to be stored for relatively long periods of time before use.

A further study for a longer period of time will be carried out. The reasons for the slower ageing of the IJ ink will also be studied. The difference in stability with time could be attributable to the different nature of the types of inks.

## Acknowledgements

This research was funded by CONICET, grant PIP 2013-2015 N 301. Special thanks are extended to Dr Andrea Berkovic for the spectrophotometer measurements.

## References

1. M. Waks Serra, N. Carbone, H. Di Rocco, H. Garcia, D. Iriarte, J. Pomarico and H. Ranea-Sandoval, "Diffuse light transmission profiles obtained using CW: a comparative analysis with time resolved experiments", *Optik Int. J. Light Electron Opt.* **125**, 3507 (2014). doi: <http://dx.doi.org/10.1016/j.ijleo.2014.02.003>
2. N.A. Carbone, G.R. Baez, H.A. Garcia, M.V. Waks Serra, H.O. Di Rocco, D.I. Iriarte, J.A. Pomarico, D. Grosenick and R. Macdonald, "Diffuse reflectance optical topography: location of inclusions in 3D and detectability limits", *Biomed. Opt. Express* **5**, 1336 (2014). doi: <http://dx.doi.org/10.1364/BOE.5.001336>
3. S. Andersson-Engels, R. Berg, S. Svanberg and O. Jarlman, "Time-resolved transillumination for medical diagnostics", *Opt. Lett.* **15**, 1179 (1990). doi: <http://dx.doi.org/10.1364/OL.15.001179>
4. S. Andersson-Engels, R. Berg and S. Svanberg, "Effects of optical constants on time-gated transillumination of tissue and tissue-like media", *J. Photochem. Photobiol. B* **16**, 155 (1992). doi: [http://dx.doi.org/10.1016/1011-1344\(92\)80006-H](http://dx.doi.org/10.1016/1011-1344(92)80006-H)
5. B. Cox, J.G. Laufer, S.R. Arridge and P.C. Beard, "Quantitative spectroscopic photoacoustic imaging: a review", *J. Biomed. Opt.* **17**, 061202 (2012). doi: <http://dx.doi.org/10.1117/1.JBO.17.6.06120>
6. B.J. Tromberg, B.W. Pogue, K.D. Paulsen, A.G. Yodh, D.A. Boas and A.E. Cerussi, "Assessing the future of diffuse optical imaging technologies for breast cancer management", *Med. Phys.* **35**, 2443 (2008). doi: <http://dx.doi.org/10.1118/1.2919078>
7. R. Choe, A. Corlu, K. Lee, T. Durduran, S.D. Konecky, M. Grosicka-Koptyra, S.R. Arridge, B.J. Czerniecki, D.L. Fraker, A. DeMichele, B. Chance, M.A. Rosen and A.G. Yodh, "Diffuse optical tomography of breast cancer during neoadjuvant chemotherapy: a case study with comparison to MRI", *Med. Phys.* **32**, 1128 (2005). doi: <http://dx.doi.org/10.1118/1.1869612>
8. A. Cerussi, N. Shah, D. Hsiang, A. Durkin, J. Butler and B.J. Tromberg, "In vivo absorption, scattering, and physiologic properties of 58 malignant breast tumors determined by broadband diffuse optical spectroscopy", *J. Biomed. Opt.* **11**, 044005 (2006). doi: <http://dx.doi.org/10.1117/1.2337546>
9. A.P. Gibson, J.C. Hebden and S.R. Arridge, "Recent advances in diffuse optical imaging", *Phys. Med. Biol.* **50**, R1 (2005). doi: <http://dx.doi.org/10.1088/0031-9155/50/4/R01>
10. G. Muehlelehner and J.S. Karp, "Positron emission tomography", *Phys. Med. Biol.* **51**, R117 (2006). doi: <http://dx.doi.org/10.1088/0031-9155/51/13/R08>
11. D. Grosenick, H. Wabnitz and B. Ebert, "Review: recent advances in contrast-enhanced near infrared diffuse optical imaging of diseases using indocyanine green", *J. Near Infrared Spectrosc.* **20**, 203 (2012). doi: <http://dx.doi.org/10.1255/jnirs.964>
12. F. Martelli, S. Del Bianco, A. Ismaelli and G. Zaccanti, *Light Propagation through Biological Tissue and Other Diffusive Media: Theory, Solutions, and Software*. SPIE, Bellingham, WA (2010).
13. P. Di Ninni, F. Martelli and G. Zaccanti, "The use of India ink in tissue-simulating phantoms", *Opt. Express* **18**, 26854 (2010). doi: <http://dx.doi.org/10.1364/OE.18.026854>
14. H. Wabnitz, A. Jelzow, M. Mazurenka, O. Steinkellner, R. Macdonald, D. Milej, N. Żotek, M. Kacprzak, P. Sawosz, R. Maniewski, A. Liebert, S. Magazov, J. Hebden, F. Martelli, P. Di Ninni, G. Zaccanti, A. Torricelli, D. Contini, R. Re, L. Zucchelli, L. Spinelli, R. Cubeddu and A. Pifferi, "Performance assessment of time-domain optical brain imagers, part 2: nEUROpt protocol", *J. Biomed. Opt.* **19**, 086012 (2014). doi: <http://dx.doi.org/10.1117/1.JBO.19.8.086012>
15. H. Wabnitz, D.R. Taubert, M. Mazurenka, O. Steinkellner, A. Jelzow, R. Macdonald, D. Milej, P. Sawosz, M. Kacprzak, A. Liebert, R. Cooper, J. Hebden, A. Pifferi, A. Farina, I. Bargigia, D. Contini, M. Caffini, L. Zucchelli, L. Spinelli, R. Cubeddu and A. Torricelli, "Performance assessment of time-domain optical brain imagers, part 1: basic instrumental performance protocol", *J. Biomed. Opt.* **19**, 086010 (2014). doi: <http://dx.doi.org/10.1117/1.JBO.19.8.086010>

16. S.J. Madsen, M.S. Patterson and B.C. Wilson, "The use of India ink as an optical absorber in tissue-simulating phantoms", *Phys. Med. Biol.* **37**, 985 (1992). doi: <http://dx.doi.org/10.1088/0031-9155/37/4/012>
17. D. Contini, F. Martelli and G. Zaccanti, "Photon migration through a turbid slab described by a model based on diffusion approximation. I. Theory", *Appl. Opt.* **36**, 4587 (1997). doi: <http://dx.doi.org/10.1364/AO.36.004587>
18. H.O. Di Rocco, D.I. Iriarte, J.A. Pomarico and H.F. Ranea-Sandoval, "Light transmittance in turbid media slabs used to model biological tissues; scaling laws", *Optik Int. J. Light Electron Opt.* **121**, 435 (2010). doi: <http://dx.doi.org/10.1016/j.ijleo.2008.07.028>
19. T. Vo-Dinh (Ed), *Biomedical Photonics Handbook*. CRC Press, Boca Raton, FL (2003).

